Supplementary Information

Chirality and Dislocation Effects in Single Nanostructures Probed by Whispering Gallery Modes

Peter Sutter, Larousse Khosravi-Khorashad, Cristian V. Ciobanu, and Eli Sutter
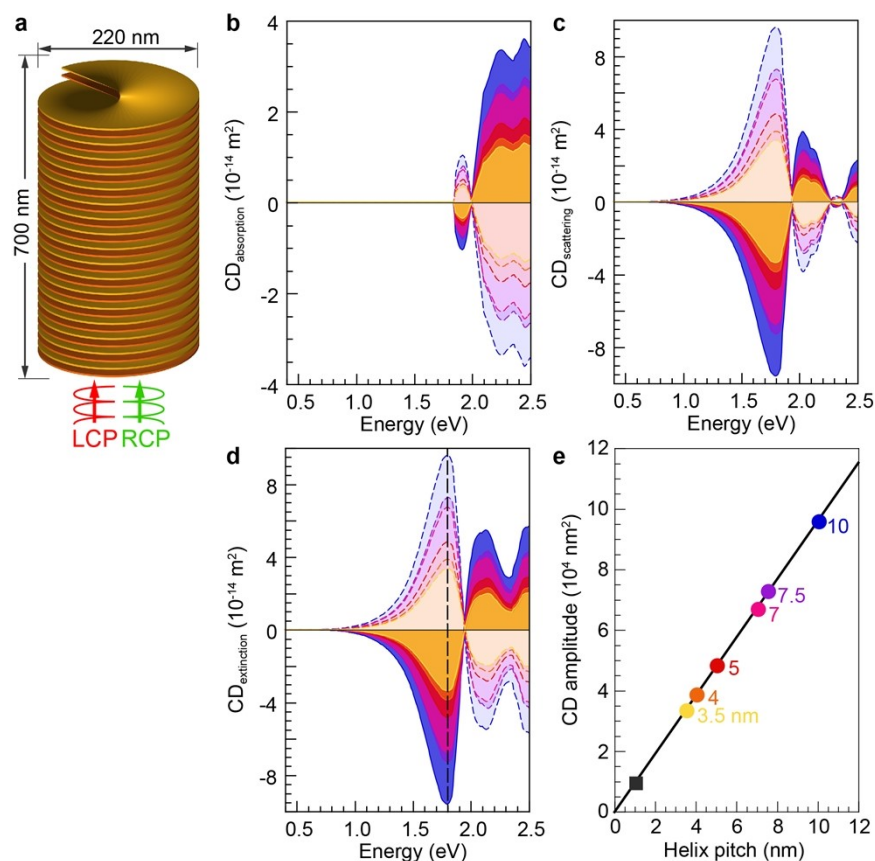
Supplementary Figures

Figure S1. Simulations of circular dichroism (CD) of helical GeS nanostructures. a. Schematic of the helical nanostructure model with axially incident left-circularly polarized (LCP) and right-circularly polarized (RCP) waves. For the simulations, a nanowire segment of 200 nm diameter and 700 nm length was modeled. Since simulating the actual helical structure with a pitch of ~1 nm (equal to the Burgers vector **b** of the axial screw dislocation) was computationally prohibitive, several geometries with larger pitch were simulated and extrapolation to a 1 nm pitch was used to determine the expected CD of our synthetic helical GeS nanostructures. **b.** Computed CD in the absorption. **c.** Computed CD in the scattering. **d.** Computed CD in the extinction. Differently colored curves in panels b. – d. correspond to different pitch of the helical nanostructure, ranging from 10 nm (blue) to 3.5 nm (yellow); solid (dark shaded) and dashed (light shaded) spectra correspond to helical GeS nanostructures with opposite handedness. **d.** Amplitude of the first peak (centered at ~1.8 eV photon energy) in the extinction CD as a function of the helix pitch (circles), and extrapolation to the 1 nm pitch of the twisted GeS nanowires (gray square).
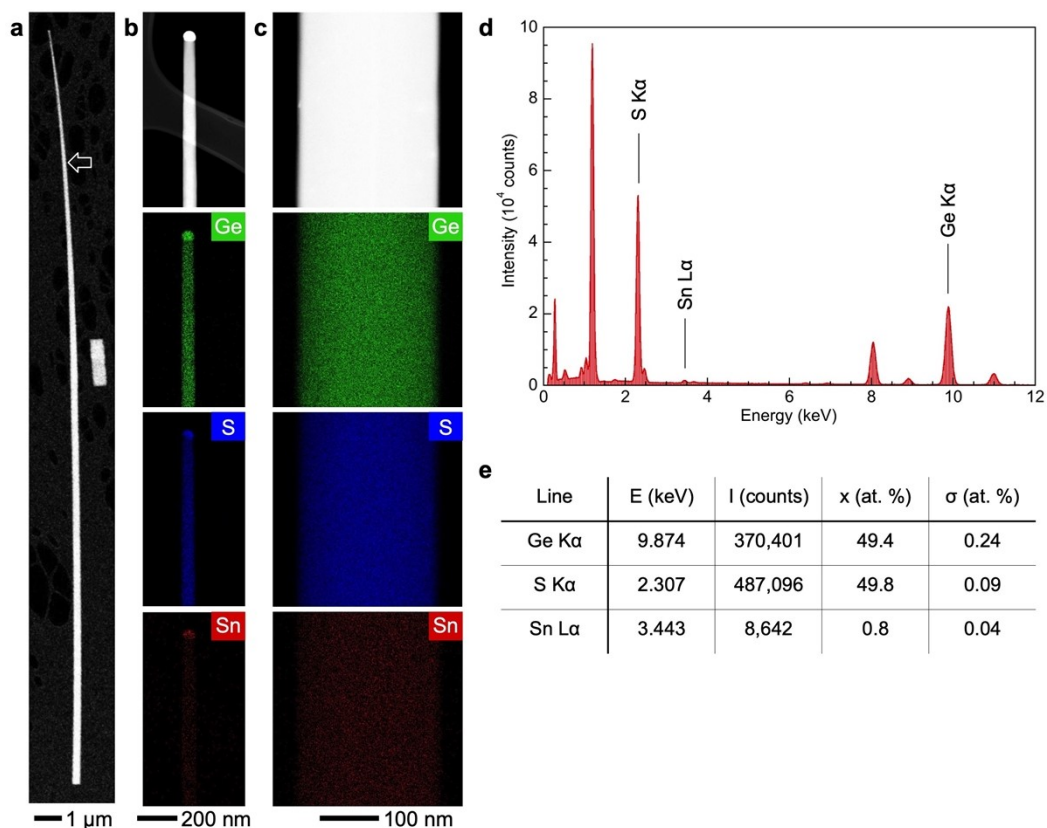
Line	E (keV)	I (counts)	x (at. %)	σ (at. %)
Ge Kα	9.874	370,401	49.4	0.24
S Kα	2.307	487,096	49.8	0.09
Sn Lα	3.443	8,642	0.8	0.04

Figure S2. Chemical mapping and composition analysis of tapered nanowires grown from mixed GeS and SnS precursors at 240°C. a. HAADF-STEM image of a characteristic tapered nanowire. **b.** STEM image (top) along with Ge, S, and Sn energy dispersive X-ray spectroscopy (EDS) maps obtained near the nanowire tip, terminated by the Au-rich VLS catalyst particle. **c.** EDS maps obtained along the wire (arrow in a.). **d.** EDS spectrum obtained at the position marked by the arrow in a. **e.** Quantification of the composition *x* of the nanowire from the EDS spectrum shown in d. σ: Standard deviation of the composition. The ratio between Ge and S is close to the expected value of 1 for GeS, whereas the Sn content is typically below 1 at. %.
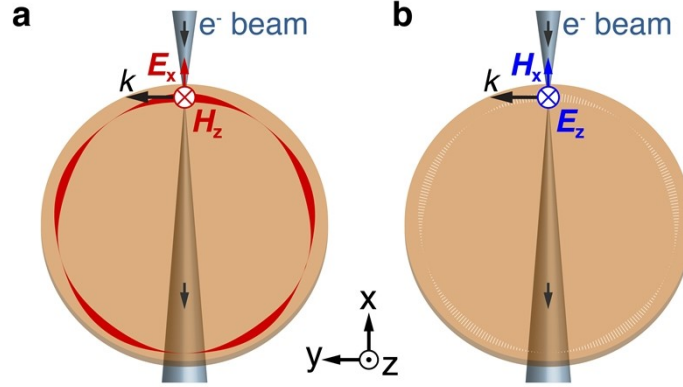
Figure S3. Electron beam excitation of WGMs in van der Waals nanowires. a. Allowed excitation of E_x polarized WGMs with electric field vector parallel to the electron trajectory. **b.** Forbidden excitation of E_z polarized WGMs, whose electric field vector is perpendicular to the electron trajectory.
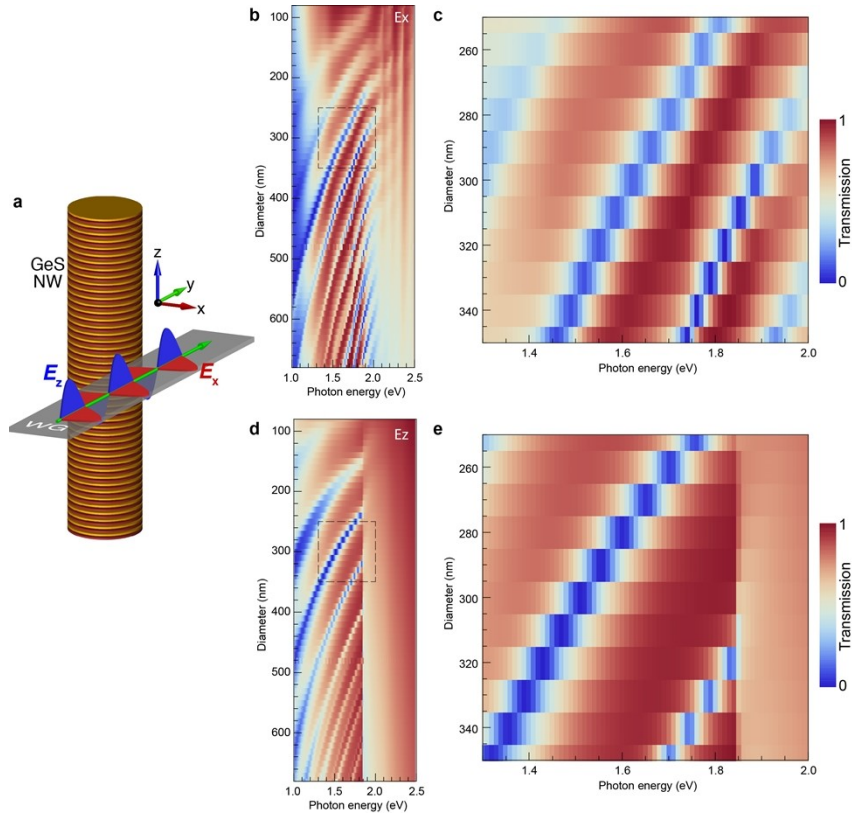

Figure S4. Numerical simulations of whispering gallery modes in achiral GeS nanowires. a. Schematic of the simulation geometry, consisting of the Ge nanowire (NW) with an adjacent strip waveguide (WG). Excitation of whispering gallery modes coincides with minima in the transmission of waveguide. We distinguished two different excitation polarizations, namely E_x (transverse electric, TE) and E_z (transverse magnetic, TM) polarization, respectively. **b.** Dispersion of WGMs with GeS nanowire diameter for E_x polarized (TE) excitation. **c.** Detail of the WGM dispersion (for E_x excitation) in the range of nanowire diameters between 250 – 350 nm. **d.** Dispersion of WGMs with GeS nanowire diameter for E_z polarized (TM) excitation. **e.** Detail of the WGM dispersion (for E_z excitation) in the range of nanowire diameters between 250 – 350 nm.
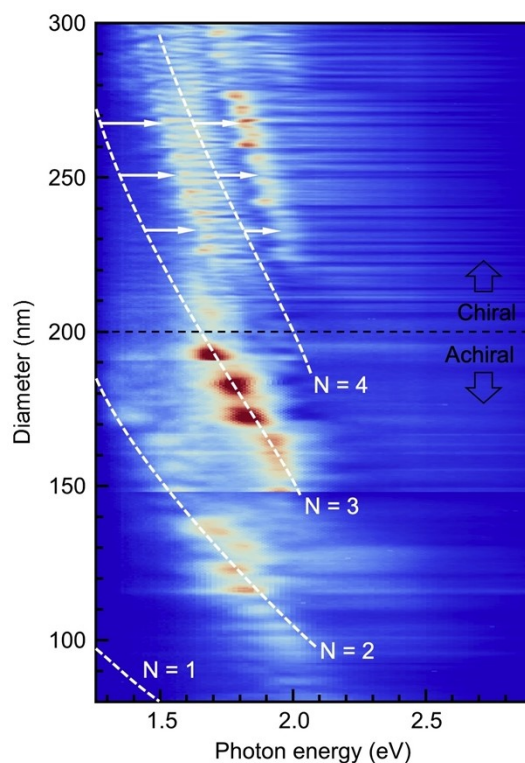
Figure S5. Transition from achiral to chiral whispering gallery modes (WGMs) in tapered GeS van der Waals nanowires. False color plot shows the measured, photon energy dependent CL intensity along the nanowire shown in Figure 2, plotted against the wire diameter. The transition between the achiral (layered) and chiral (twisted) segment of the wire is marked by a horizontal dashed line (at ~200 nm diameter). Dashed white lines denote the predicted WGM dispersions of N = 1 to N = 4 modes, calculated using a plane wave model based on the published optical constants of GeS. Note the close correspondence between the calculated and measured mode energies in the achiral segment, and the consistent blue shift of the observed modes in the chiral segment of the wire (white arrows).
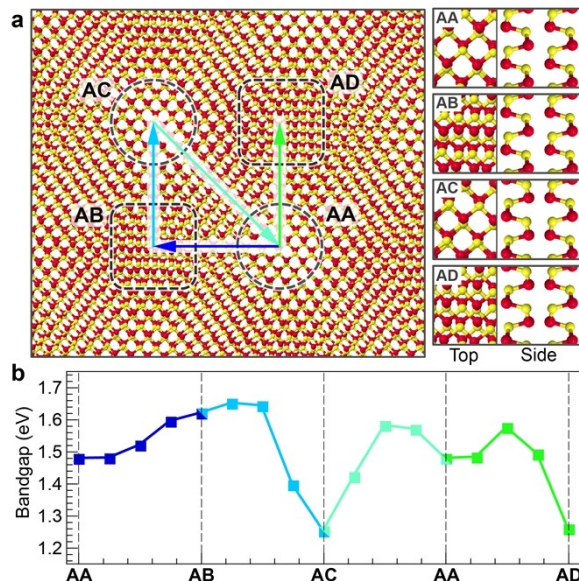
Figure S6. Density functional theory (DFT) calculations of the energy landscape across the GeS twist moiré. a. Illustration of the different moiré registries for the example of an interlayer twist angle of 4°. **b.** DFT calculated bandgaps along the colored lines between different moiré registries shown in a. To simplify the calculations, we approximated the continuously changing registry of the twist moiré between adjacent GeS layers (panel a.) *via* a series of linear shifts (an excellent approximation for the small twist angles realized here; see Supplementary Figure 6). Since calculations using GGA functionals underestimate the bandgaps, we applied a correction by scaling the gap in regions with AB equilibrium bulk stacking to the experimentally observed value (~1.62 eV, see Figure 4a).
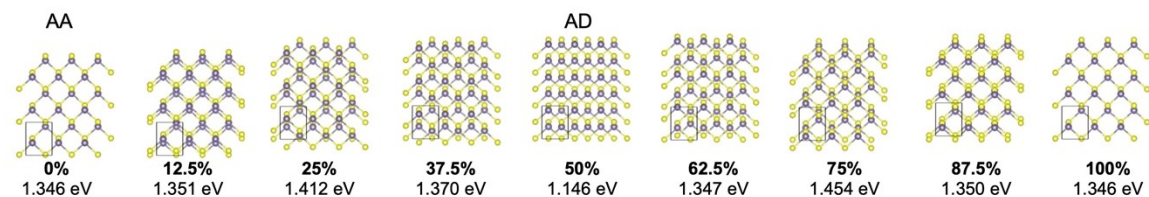
a. Shift along *a*-axis
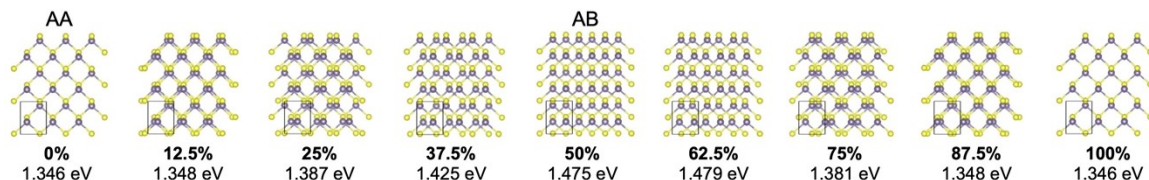
b. Shift along *b*-axis

Figure S7. Linear shifts to simulate different moiré registries in DFT bandgap calculations. a. Progressive shifts along the *a*-direction (blue arrow in Supplementary Figure 5). **b.** Progressive shifts along the *b*-direction (green arrow in Supplementary Figure 5). Energies represent the raw (GGA calculated) bandgap values prior to correction of the AB stacked region to match the experimentally observed bandgap.
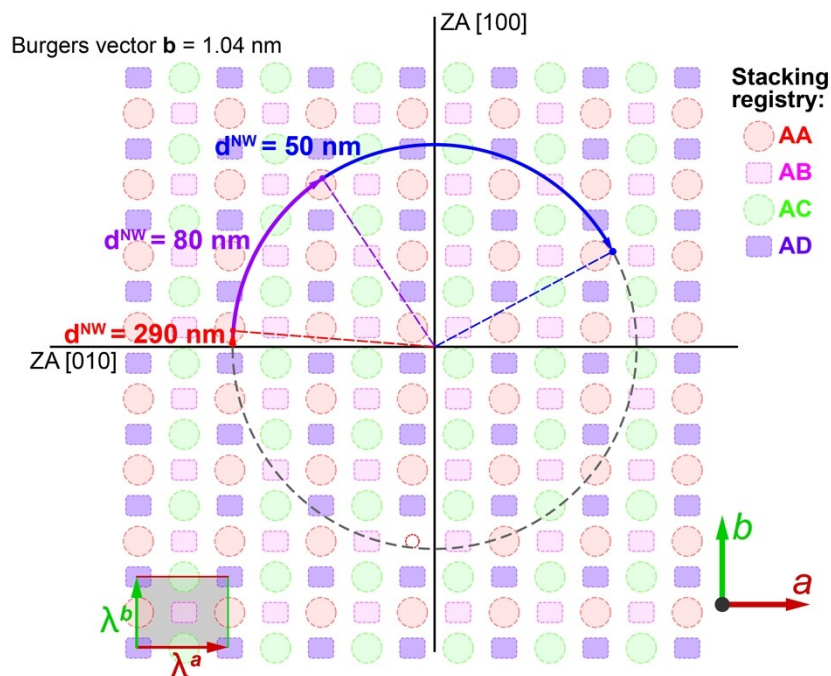
Figure S8. Comparison of the moiré registries traversed along a 5 µm long GeS nanowire section for thin (50 nm), intermediate (80 nm) and thick (290 nm) wires. While a 5 µm section of a thin (50 nm) wire covers a cumulative twist of ~150°, for thicker (80 nm) wires this value is reduced to 56°, and for the thick (290 nm) wires considered here it is further reduced to 4.5°. Hence, for the same Burgers vector (**b** = 1.04 nm), a 5 µm section of a thin (50 nm) wire contains transitions between many different moiré registries (blue arc). For a thicker (80 nm) wire, the number is reduced to just a few (purple arc). For a thick (290 nm) wire, a 5 µm long segment will contain only a single moiré registry (red arc).
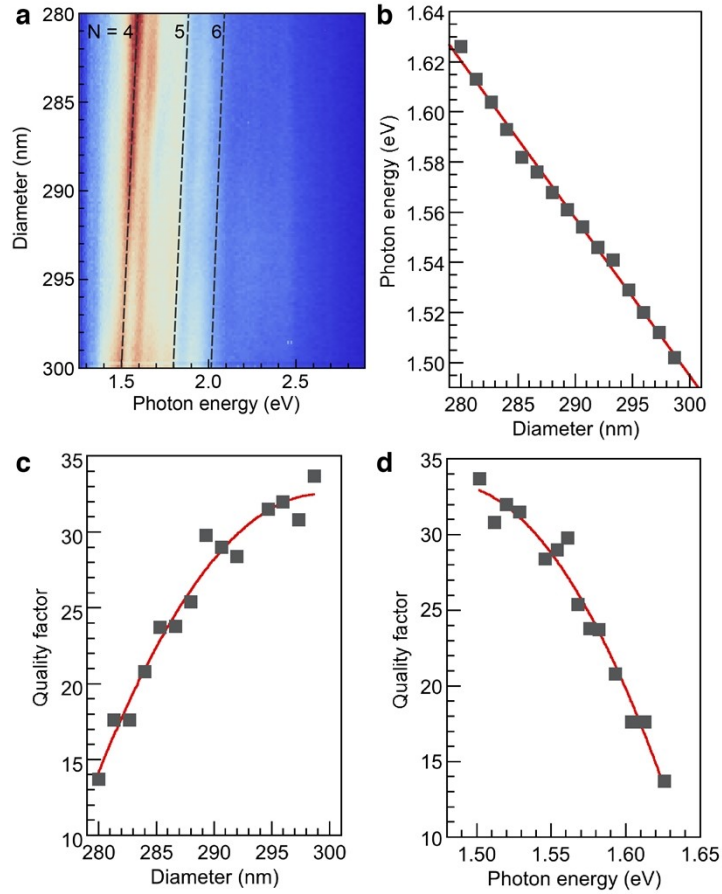
Figure S9. Energy dependent quality factor of the *N* = 4 WGM in a defect-free GeS nanowire. a. Hyperspectral CL linescan along a section of the tapered nanowire ranging in diameter from 280 nm to 300 nm. **b.** Diameter dependent energy of the WGM, obtained from Gaussian fits to the CL spectra. **c.** Quality factor, determined *via* Q = Δ(hv)/hv, where hv is the photon energy and Δ(hv) the full-width at half maximum of the emission peak corresponding to the *N* = 4 WGM. **d.** Quality factor as a function of photon energy, showing the decrease in the quality factor (*i.e.*, increase in spectral linewidth) as the photon energy approaches the GeS bandgap.
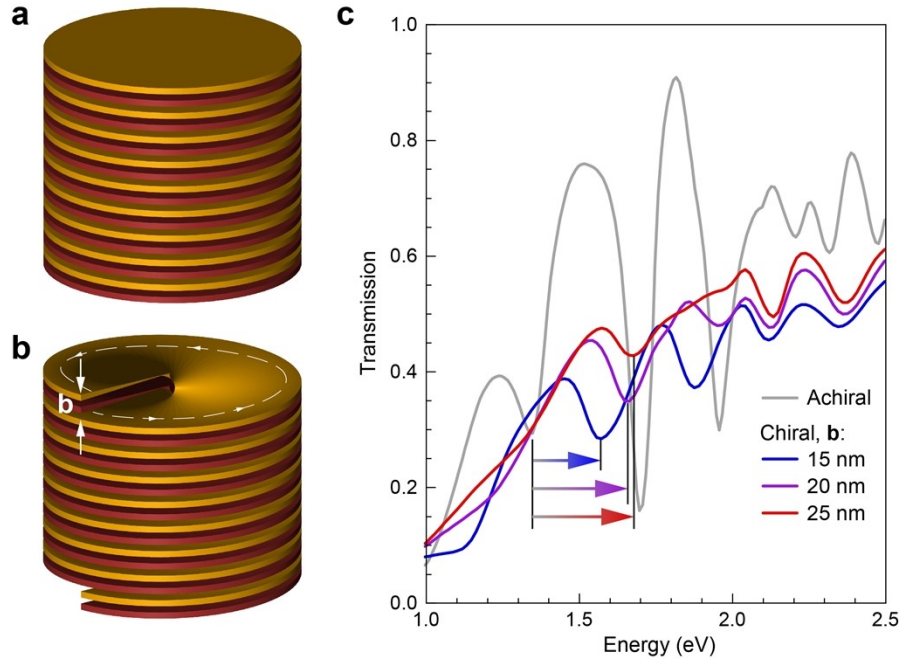
Figure S10. Dependence of the spectral blue shift of whispering gallery mode (WGM) on the Burgers vector (helix pitch) in chiral nanowires. a. Schematic illustration of an achiral van der Waals nanowire. **b.** Illustration of a dislocated, chiral wire with screw dislocation Burgers vector (*i.e.*, helix pitch), b. **c.** Comparison of Comsol simulations of the transmission of a strip waveguide exciting WGMs (as shown in Figure 3 of the main text) in an achiral wire, as well as chiral wires with helix pitch of 15 nm, 20 nm, and 25 nm, respectively. The wire diameter in all four cases is 280 nm. Note the progressive increase in the WGM energy (*e.g.*, for the mode with ~1.35 eV energy in the achiral wire) with increasing pitch of the helical structure (arrows).